Palaeogeography, Palaeoclimatology, Palaeoecology 511 (2018) 419–432

Contents lists available at ScienceDirect

Palaeogeography, Palaeoclimatology, Palaeoecology

journal homepage: www.elsevier.com/locate/palaeo

Miocene pollen assemblages from the Zeku Basin, northeastern Tibetan Plateau, and their palaeoecological and palaeoaltimetric implications

Zhengchuang Hui[a,*], Xiangchuan Li[b,c], Zhenhua Ma[a], Liang Xiao[b], Jun Zhang[a], Jing Chang[a]

[a] Key Laboratory of Western China's Environmental Systems (Ministry of Education), College of Earth and Environmental Science, Lanzhou University, Lanzhou 730000, China

[b] School of Earth Sciences and Resources & Key Laboratory for the Study of Focused Magmatism and Giant Ore Deposits, MLR, Chang'an University, Xi'an 710054, China

[c] State Key Laboratory of Palaeobiology and Stratigraphy, Nanjing Institute of Geology and Palaeontology, Chinese Academy of Sciences, Nanjing 210008, China

ARTICLE INFO

Keywords:
Palaeovegetation
Climate change
Temperature lapse rate method
Miocene elevation

ABSTRACT

A comprehensive understanding of the tectonic uplift history of the Tibetan Plateau (TP), a 2000 km wide region with a mean altitude of 4000–5000 m above sea level (asl), is crucial for interpreting global Cenozoic climate change, collisional tectonics and the evolution of the Asian climatic system. However, the timing, degree and extent of the uplift of the TP remain controversial. Here we report new palynological data from Early to Mid-Miocene lacustrine-swamp sediments in the Zeku Basin, northeastern TP. The palynoflora includes 68 palynotaxa at a family or genus level, comprising gymnosperms (16.2%), angiosperms (77.9%), pteridophytes (2.9%) and others (2.9%), and is suggestive of a mixed warm temperate forests of coniferous (*e.g.*, *Picea*, *Abies* and *Tsuga*) and deciduous broadleaved trees (*e.g.*, *Ulmus/Zelkova*, *Betula* and *Quercus*), with some subtropical elements (*e.g.*, *Carya* and *Liquidambar*). Three periods of vegetation succession can be recognized from the Caergen Section, indicating a stepwise warming and drying trend from bottom to top. The local palaeoclimatic parameters obtained by applying the Coexistence Approach (CoA) to palynologic assemblages rendered mean annual temperature (MAT) values of 14.2–16.1 °C and mean annual precipitation (MAP) values of 797–1113 mm. This study departs from the traditional application of the CoA, relying on published determination of plant-climate relationships, rather than on data derived from the Paleoflora Database, which is currently not fully open-access. Based on the difference in temperatures between the Early to Mid-Miocene and the present day, and the temperature lapse rate, corrected to take account of Miocene global temperature differences, the estimated palaeoaltitude of the Zeku Basin during the Early to Mid-Miocene was 1200–1400 m asl. This palaeoaltitude estimate suggests that this basin has experienced about 2200–2500 m of uplift since the Early to Mid-Miocene. Findings therefore do not support previous hypotheses that the northeastern TP attained its present altitude before the Miocene.

1. Introduction

The uplift of the Tibetan Plateau (TP), the highest and largest plateau in the world, has not only changed the environment of the plateau region itself, but has also exerted a tremendous influence on the climate of Asia (*e.g.*, the Asian monsoonal climate and the aridity of the continental interior) through the dynamic and thermal conditions present during the Cenozoic (Manabe and Terpstra, 1974; Kutzbach et al., 1989; An et al., 2001; Wu et al., 2006; Boos and Kuang, 2010; Li, 1995; Li et al., 2014a, 2014b).

Modeling studies have shown that the surface uplift of the TP may have led to zonal atmospheric circulations (*e.g.*, the Westerlies) being deflected around the TP (Ruddiman and Kutzbach, 1989). Furthermore, this deflection may have resulted in the development of seasonal precipitation patterns in Asia (Molnar et al., 2010). It has been suggested that the degree and extent of the surface uplift of the TP can be constrained from any climatic changes resulting from plateau growth (Kutzbach et al., 1989; Ruddiman and Kutzbach, 1989; Hsu and Liu, 2003). Therefore, it is scientifically reasonable to suggest that characterizing such palaeoclimatic changes and their patterns in space and time will help delineate the uplift history of the TP. Furthermore, the palaeoaltimetry of the TP as deduced from palaeoclimatic changes resulting from plateau uplift may be more reliable compared to other evidence, such as estimated obtained from single tectonic events.

Currently, there are many different opinions regarding the TP's palaeoaltitudinal history. Based on isotopic evidence, the southern,

* Corresponding author.
E-mail address: huizhch@lzu.edu.cn (Z. Hui).

https://doi.org/10.1016/j.palaeo.2018.09.009
Received 1 December 2017; Received in revised form 6 September 2018; Accepted 6 September 2018
Available online 12 September 2018

central and northern TP reached, or exceeded, its present-day altitude by the Miocene, Oligocene or Eocene, and Mid-Eocene, respectively (Currie et al., 2005; Garzione et al., 2000; Rowley et al., 2001; Rowley and Currie, 2006; Decelles et al., 2007; Quade et al., 2011). Mammalian fossils suggest that the southern TP gained its present-day altitude during the Mid-Pliocene (Deng et al., 2012), whereas palaeobotanic evidence indicates that the northern TP has been uplifted by ~2000–3000 m over the last 17 Ma (Sun et al., 2015). The geographically-extensive area that constitutes the TP, and the different methods used by authors to estimate palaeoaltitude may be responsible for these different viewpoints. Such a variety of suggestions would suggest that a method to reconstruct palaeo-altitude is needed from regions in and adjacent to the TP in order to cross-validate and test any existing theories.

The northeastern TP, bounded by the Haiyuan Fault and the Liupan Mountains to its northeast and east, the complex of Altyn Tagh faults and the Qilian Mountains to its northwest and north, and the Western Qinling and Kunlun faults to its south (Wang et al., 2011; Wang et al., 2012), is regarded as the most promising region for scientific efforts to decipher the uplift history of the TP, and any associated palaeoclimatic changes (Molnar, 2005; Molnar et al., 2010). This is because this region represents a part of the TP which has suffered, and is still suffering, active tectonic deformation (Yin et al., 1994; Meyer et al., 1998; Tapponnier et al., 2001; Lease et al., 2007; Wang et al., 2011). As a result, it is highly sensitive to climate change (Li and Feng, 1988).

Regional vegetation distribution patterns and their evolutionary history can potentially reflect any changes in the continental climate, and can also be strongly impacted by palaeogeomorphological settings (Wu et al., 1980; Wang, 1992). The palaeovegetation cover and corresponding palaeoenvironment of a region can be reconstructed using plant fossils (such as sporopollen, fruits, seeds and leaves). In recent years, palaeovegetation and palaeoclimatic parameters have been reconstructed using Neogene micro- and mega-floras, mainly in eastern China (Liang et al., 2003; Yang et al., 2007; Xu et al., 2008; Li et al., 2009; Yao et al., 2011; Xing et al., 2012; Zhang et al., 2012). However, the quantitative palaeoclimatic data derived from plant fossils in inner Asia, including from the northeastern TP, are few in comparison to the abundant data available for Chinese Cenozoic floras (Ma et al., 1998, 2005; Wu, 2001; Wang and Deng, 2009; Wu et al., 2010; Dong et al., 2011; Hui et al., 2011; Miao et al., 2013).

In this study, we analyze spore and pollen samples from Miocene sediments in the Zeku Basin, northeastern TP (Fig. 1A and B). Based on the obtained palynological data, we reconstruct the palaeovegetation and palaeoclimate of the Zeku Basin. To obtain the climatic parameters, the Coexistence Approach (CoA; Mosbrugger and Utescher, 1997) is used. Rather using data from the Palaeoflora Database, as traditionally used in CoA studies, our climate-vegetation reference dataset comes from Fang et al. (2009), for trees and shrubs, and the online database from the Chinese Virtual Herbarium (www.cvh.org.cn), and is fully open-access. The change in altitude from the Miocene to the present day on the northeastern TP is quantitatively estimated based on the difference between the obtained Miocene palaeotemperatures and the modern climatic parameters of the Zeku Basin.

2. Locality, materials and methods

2.1. The study site

The Zeku Basin, with a mean altitude of 3440–4300 m asl, is located in the eastern part of Qinghai Province, northeastern TP (Fig. 1A). The studied section, *i.e.* the Caergen Section (34°56′N, 101°48′E, 3690 m asl), is situated in Caergen Village, 30 km southeast of the administrative seat of Zeku County (Fig. 1B). The section is ~20 m deep and is a natural profile which has been exposed along the banks of the small, local stream. This section is mainly composed of mudstone, with interbedded layers of oil shale and gypsum. Its lower part consists of 265 cm of dark gray mudstone, with interbedded layers of oil shale; its middle part consists of ~665 cm of light dark gray mudstone, with increasing gypsum content; and its upper part consists of ~310 cm of khaki calcareous mudstone, with interbedded layers of shale and gypsum (for details see Fig. 2 and Supplementary Table S1).

The oil shale layers of the lower part of the Caergen Section have yielded abundant exquisitely-preserved plant and animal fossils, *i.e.*, of different species of wood, seeds, fruit, insects, arachnids, as well as bird feathers (Young, 1975; Guo, 1980; Li et al., 2013a, 2013b, 2014a, 2014b, 2016; Fig. 2). We only sampled the lower 11.24 m of the Section, as its upper part of ~10 m is too weathered to obtain reliable data. Based on a drilling report from a regional geologic survey and an evaluation of local ore resources, this stratigraphic suite has been assigned to the Miocene (SCQPWG (Stratigraphic Charts of Qinghai Province Writing Group), 1980). According to recent high-resolution magnetostratigraphic work from the nearby Guide Basin, the fossil-bearing oil shale layers from the Caergen Section are equivalent to the upper part of the Garang Formation (< 16–19 Ma) (Fang et al., 2007; Li et al., 2016). This would indicate that the age of this Section should be constrained to the Early to Mid-Miocene (Fang et al., 2005, 2007; Li et al., 2016).

At present, the northeastern TP experiences a typical continental plateau monsoonal climate. In terms of climatic division, the region belongs to the subnival humid plateau climatic zone (Zhou et al., 1987). The MAT and MAP of this region are ~−2.6 °C and ~460 mm, respectively, with most rainfall during the summer months. The mean annual evapotranspiration is ~1325 mm, almost three times the MAP value (IDBMC (Information Department of Beijing Meteorological Center), 2004).

The present-day natural vegetation of this region is steppe alpine meadow, in which the dominant species is *Kobresia pygmaea*, with secondary species being *K. humilis*, *K. bellardii*, *K. prattii*, *Carex atrofusca*, *Potentilla nivia*, *Gentiana dahurica*, *Leonopodium nanum*, *Thalictrum alpinum*, *Saussurea superba*, *Taraxacum mongolicum*, *Polygonum viviparum*, *Anaphalis lacteal*, *Lancea tibetica*, *Oxytrapis kansuensis*, *Iris potaninii*, *etc*. (Zhou et al., 1987).

2.2. Materials and palynological methods

Based on the observed lithologic division (Supplementary Table S1), 65 sediment samples were taken from the Caergen Section for palynologic analysis (Fig. 2). In the laboratory, and according to the noted lithology, 10–30 g of each sample were crushed and then treated consecutively with 10% and 39% HF to remove carbonates and silica. The residue was then sieved through a 10 μm mesh of nylon cloth in an ultrasonic bath. If the impurities in the remains were too many to identify, we then used a heavy liquid ($ZnCl_2$, density: 1.8 g/ml) to concentrate the spores and pollen. Finally, the residues were stored in a 10 ml plastic test tube for identification.

Identification of the spore and pollen grains was conducted under an Olympus light microscope, usually set to a 400× magnification, and based on comparisons with published modern and fossil pollen atlases (Wang et al., 1995; Song et al., 1999), as well as modern pollen slides preserved in the Geography Department of Lanzhou University. Usually, > 300 specimens were counted per sample. Pollen diagrams were prepared using Tilia software (Grimm, 1991). All the processed samples are housed at the College of Earth and Environmental Sciences, Lanzhou University, Gansu Province, China.

2.3. Coexistence approach

We employed the CoA method developed by Mosbrugger and Utescher (1997) for quantitative palaeoclimatic reconstructions of the Zeku Basin area. The principle behind this method is that the climatic tolerances/requirements of a fossil plant are same, or similar, to its nearest living relatives (NLRs) if its modern affinities can be determined

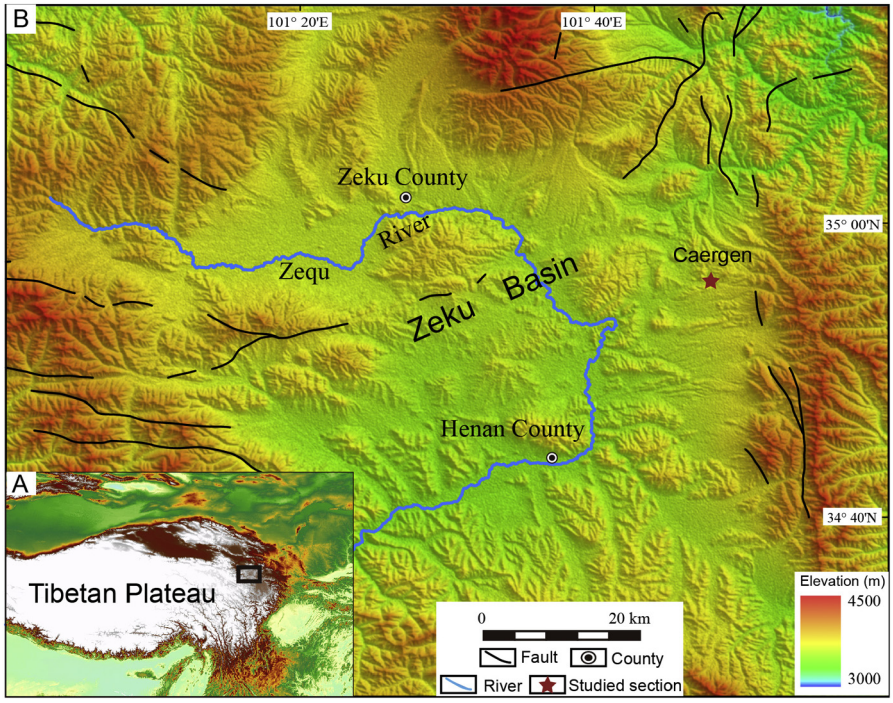

Fig. 1. Location of the Zeku Basin in the Tibetian Plateau region, and the study site at Caergen (DEM data from https://earthdata.nasa.gov/).

(Mosbrugger and Utescher, 1997). For a given fossil plant assemblage, such as palynoflora, the "coexistence interval" of each climatic parameter is determined using the climatic tolerances of its corresponding NLR, therefore representing the climatic conditions of the given fossil location during a specific geologic period (Mosbrugger and Utescher, 1997; Utescher et al., 2014). This method is widely used in Europe and Asia because it is organ-independent and can be applied to both macro- (leaf, fruits and seeds, *etc*.) and micro-plant fossils (pollen and spores) (Mosbrugger et al., 2005; Kou et al., 2006; Bruch and Zhilin, 2007; Utescher et al., 2011; Quan et al., 2012; Zhang et al., 2012; Vieira et al., 2018; Srivastava et al., 2018; Prasad et al., 2018; Li et al., 2018). Following the procedure (Kou et al., 2006; Utescher et al., 2014), seven climatic parameters, *i.e.*, MAT, mean temperature of the warmest month (WMT), mean temperature of the coldest month (CMT), the difference in temperature between the coldest and warmest month (DT), MAP, mean maximum monthly precipitation (MaMP) and mean minimum monthly precipitation (MiMP), were delineated.

It should be mentioned that the CoA has been recently challenged by Grimm and Denk (2012), Grimm and Potts (2016) and Grimm et al. (2016). According to their studies, the main sources of error of CoA are problems in determining minimum-maximum climate tolerances of taxa used as NLRs, incorrect associations of fossil taxa with NLRs, and taxonomic uncertainties (*e.g.* Grimm and Denk, 2012; Grimm and Potts, 2016; Grimm et al., 2016). Based on their work on modern flora to reconstruct the mean annual temperature (MAT), the CoA was referred to as "useless" for quantitative reconstruction of palaeoclimate (Grimm and Denk, 2012). However, this conclusion drawn from the results presented there may be still debated.

Although Grimm and Denk's (2012) work uncovered some erroneous entries regarding climatic ranges (*e.g.* related to minimum-maximum climate tolerances of taxa used as NLRs) of extant plant taxa in the Palaeoflora Database (Utescher and Mosbrugger, 1997–2012), these did not arise from deficiencies in the CoA method itself. Furthermore, this study is not qualified to assess the reliability of the CoA, because the authors use the unspecific climate dataset to reconstruct very specific climate conditions. For example, the authors use climate data for plant families to reconstruct the climate of the Alpine zone in Georgia in which lower taxonomic level (*genus*) plants are distributed. In fact, the Palaeoflora database is checked and updated in regular intervals (Utescher and Mosbrugger, 2012).

Theoretically, the older the age of fossils, the greater the uncertainties to determine its NLRs. According to the Cenozoic vegetation evolution in China, the vegetation belt distribution was similar to present since the early Miocene (Neogene) (Wu et al., 1980; Wang, 1994; Song et al., 1999; Sun and Wang, 2005). This implies that a close affinity with their modern analogs and no significant change in environmental requirements of any taxon are expected (Chaloner and Creber, 1990; Mosbrugger, 1999). Thus, the CoA is suitable to reconstruct palaeoclimate conditions since Neogene.

It should be pointed that the reliability of the CoA has been proved by other methods such as Climate Leaf Analysis Multivariate Program (CLAMP) and Leaf Margin Analysis (LMA) on the same fossil flora (Liang et al., 2003), and marine oxygen isotope records (Mosbrugger et al., 2005). The down to date studies in Europe and Asia which have employed the CoA (Vieira et al., 2018; Srivastava et al., 2018; Prasad et al., 2018; Li et al., 2018) also show that, although this method needs to be improved to some extent, it is still very useful for reconstructing Cenozoic climatic changes in East Asia.

2.4. Data accessibility for CoA determinations

Another major category of problem for applying the CoA is that the evidential basis of modern plant-climate relationships in Palaeoflora Database is not open-access at the time of writing. This creates raises problems for scientists who wish to check the reproducibility of studies. To circumvent this problem, in this study, plant distribution and climate information comes directly from Fang et al. (2009), rather than from the Palaeoflora Database, for trees and shrubs, and the online database from the Chinese Virtual Herbarium (www.cvh.org.cn) is used for non-trees, to reconstruct the palaeoclimate in this study.

In addition, all of the pollen and spores fossils' NLRs determination is based on the published literature (Song et al., 1999). In order to reduce the chance for taxonomic identification errors that may occur between different palynologists, all of the sporopollen samples were analyzed by the corresponding author, and by operators from the same laboratory. As regarding the difficult indistinguishable pollen, such as

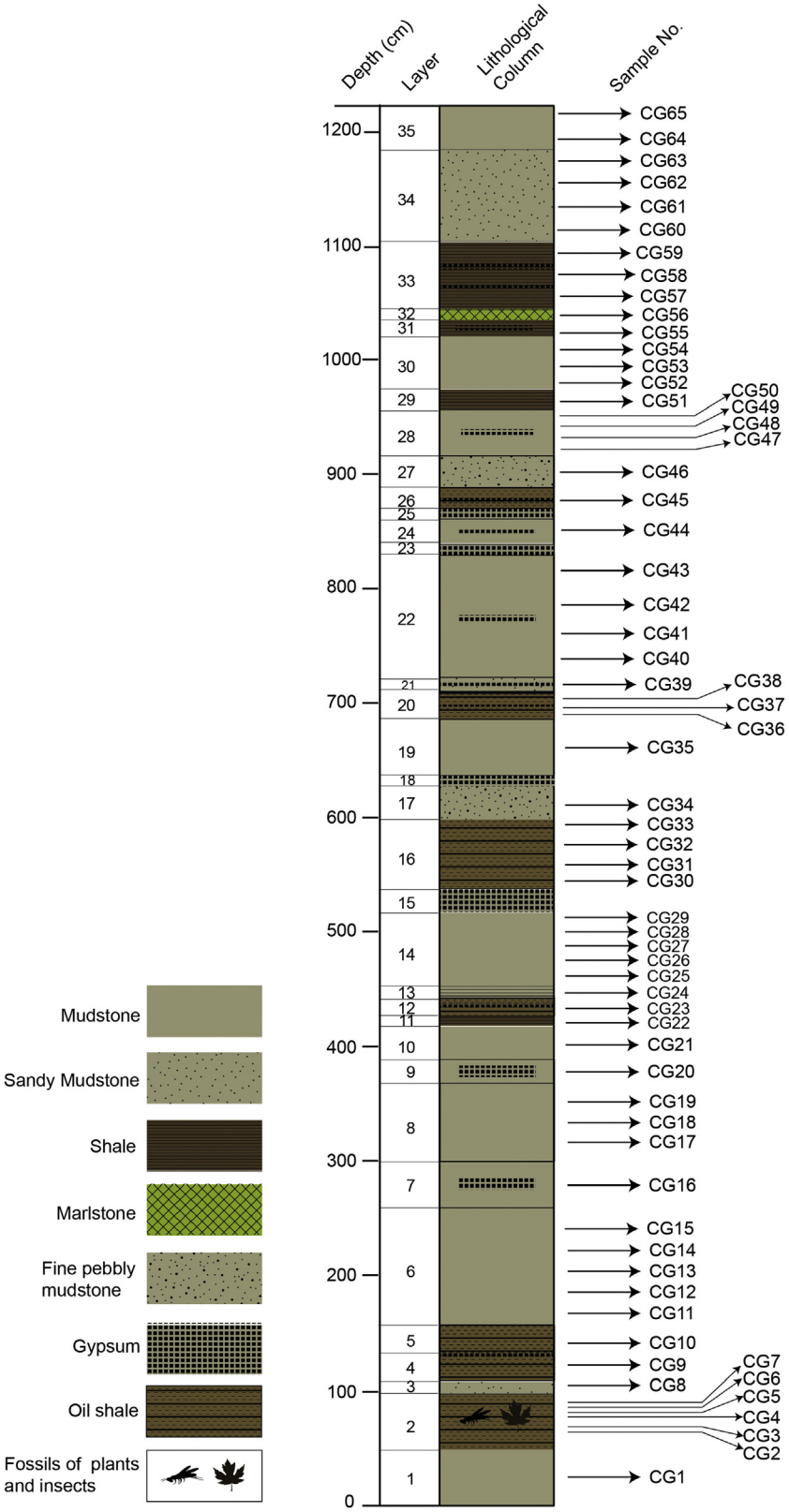

Fig. 2. The measured stratigraphic sequence at the Caergen Section, showing the position of the sampled horizons.

the Cupressaceae pollen grains (Grimm et al., 2016; Grimm and Potts, 2016) were not involved in the CoA analysis. The results of this study show that climatic ranges of all taxa involved in the CoA analysis show overlapping, implying that a consistent reconstruction of the past climate is obtained.

3. Results

3.1. Palynologic assemblages

All of the 65 palynologic samples yield abundant pollen and spore

Table 1
List of the Early Miocene Caergen Section palynomorph taxa grouped by ecologic requirements, and their relative abundances in each of the three zones (table style refers to Jiménez-Moreno, 2006).

Zone	1 (%)	2 (%)	3 (%)	Zone	1(%)	2 (%)	3 (%)
Megathermic elements				*Larix*	0.03	0.35	0.5
Sapindaceae	/	0.03	0.04	*Abies*	6.2	0.85	1.5
Mega-mesothermic elements				Non-significant elements			
Liquidambar	0.07	0.02	0.11	Rosaceae	0.08	0.46	0.96
Podocarpus	0.69	0.38	0.24	Indet. grains	0.84	5.6	6.9
Meliaceae	0.08	0.06	0.04	Shrubs & herbs			
Magnoliaceae	/	/	0.02	Ericaceae	/	/	0.02
Euphorbiaceae	/	/	0.02	Liliaceae	/	0.01	/
Cedrus	0.12	0.07	0.1	Leguminosae	/	0.07	0.16
Keteleeria	/	0.01	0.02	*Humulus*	/	0.1	0.9
Mesothermic elements				Labiate	0.54	1.88	2
Ginkgo	/	0.03	0.07	Polygnoaceae	/	0.03	0.04
Ulmus/Zelkova	21.59	26.96	24.76	Cruciferae	/	0.14	0.18
Celtis	0.11	0.25	0.23	Umbelliferae	/	0.01	/
Quercus	0.15	1.82	2.27	Amaranthaceae	0.04	0.04	0.13
Castanea	0.07	0.02	0.11	Dipsaceae	/	/	0.06
Acer	0.91	0.82	1.06	Ranunculaceae	0.15	0.17	0.21
Betula	2.49	19.53	12.7	Chenopodiaceae	0.83	12.37	16.83
Alnus	0.23	0.80	0.91	*Artemisia*	0.18	0.04	0.09
Carpinus	0.5	0.53	0.87	Poaceae	0.23	0.36	1.15
Betulaceae	/	0.3	0.02	Asteraceae	0.4	0.04	0.27
Momipites	0.08	/	/	*Nitraria*	0.07	0.17	0.34
Juglans	0.28	0.22	0.26	*Ephedra*	0.48	0.97	2
Carya	0.21	0.09	0.67	*Typha*	0.11	0.01	0.08
Pterocarya	0.38	0.19	0.5	Cyperaceae	/	0.01	/
Juglandaceae	/	0.28	/	*Potamogeton*	2.6	2.87	3.33
Rhus	0.32	0.22	0.24	*Myriophyllum*	0.15	0.36	0.04
Tilia	/	0.03	/	Pteridophytes			
Oleaceae	/	0.18	0.12	Polypodiaceae	0.17	0.15	0.11
Fraxinus	0.07	0.34	0.41	Osmundaceae	/	0.09	/
Salix	0.04	0.34	0.23	Alga			
Buxus	/	0.02	/	*Concentricystes*	/	0.02	0.02
Ilex	/	0.07	0.12	Other elements			
Elaeagnlaceae	/	0.03	0.02	*Fupingopollenites*	3.1	0.7	0.93
Caprifoliaceae	0.11	0.05	0.08	*Triletes*	0.27	0.51	0.48
Meso-microthermic elements				*Tricolpopollenites*	1.13	0.6	0.72
Pinus	1.7	1.42	1.54	*Retitricolpollenites*	0.07	0.24	0.4
Tsuga	4.44	1.33	0.85	Unidentified	0.15	1.29	1.57
Microthermic elements							
Picea	50.3	16.2	12.7				

grains (each slide has > 300 grains), which can be assigned to 68 different palynomorphs (Table 1) at a family or genus level, including 11 taxa of gymnosperms (*e.g.*, *Pinus*, *Abies*, *Cedrus*, *Larix*, *Keteleeria*, *Podocarpus*, *Tsuga*, T-C-T, *Ephedra* and Pinaceae), 53 taxa of angiosperms, such as *Ulmus/Zelkova*, *Quercus*, *Acer*, *Betula*, *Alnus*, *Juglans*, Chenopodiaceae and Poaceae, two taxa of pteridophytes (*i.e.*, Polypodiaceae and Osmundaceae), one taxon of alga (*i.e.*, *Concentricystes*) and fungi. The major palynomorphs are shown in Figs. 3–4.

Based on the variations in the relative abundances of main and important pollen types, the sporopollen diagram of the Caergen Section is divided into three zones from the bottom up using the CONISS algorithm embedded in the Tilia software (Grimm, 2011; Figs. 5 and 6).

3.1.1. Zone 1

This comprises samples 58–65 inclusive (eight samples) in a 110 cm thickness of sediment. It includes 42 types of palynomorphs, comprising nine gymnosperms, 32 angiosperms (of which 12 were herbaceous), and one pteridophyte (Table 1).

The relative abundance of gymnosperm pollen is ~64.8%, of which *Picea* (12.5–84.5%) and *Abies* (1.2–14.3%) were the dominant taxa, although *Tsuga* (1.6–16.1%), *Pinus* (0–5.6%) and *Podocarpus* (0–1.6%) were also found. The angiosperm pollen contributed 30.2% of the total content, of which broadleaved trees and herbs represented 27.6% and 2.6%, respectively. Of the broadleaved trees, *Ulmus/Zelkova* (5.1–62.1%) and *Betula* (0–5.9%) were the dominant families. The relative abundance of herbs was the lowest for the whole Section. The relative abundance of extinct *Fupingopollenites* (0.8–8.3%) was also marked in this zone. Aquatic or wetland plants like *Potamogeton* (2.6%) and *Typha* (0.1%) were low in abundance, and stable throughout the Section. The most common fern was Polypodiaceae, with a relative abundance of 0.2%.

No megathermic element was observed in this zone. There were three mega-mesothermic elements (*i.e.*, *Liquidambar*, Meliaceae and *Cedrus*), 16 mesothermic elements (*e.g.*, *Ulmus/Zelkova*, *Betula*, *Acer* and *Carpinus*), two meso-microthermic elements (*i.e.*, *Pinus* and *Tsuga*), three microthermic elements (*i.e.*, *Abies*, *Picea* and *Larix*), one non-significant element (*i.e.*, Rosaceae), 12 herbs and shrubs (*e.g.*, Chenopodiaceae, *Ephedra*, Labiate and *Artemisia*) in this zone (Table 1).

3.1.2. Zone 2

This comprises samples 14–57 inclusive (44 samples) in a 905 cm thickness of sediment. It includes 62 types of palynomorphs comprising ten gymnosperms, 49 angiosperms (19 types were herbaceous), two pteridophytes, and one alga (Table 1).

In comparison with Zone 1, the relative abundance of gymnosperms (27.2%) decreased sharply, mainly as a result of the contribution made by *Picea* (0.6–49.7%). The relative abundance of angiosperm pollen (68.9%) increased markedly, principally in response to the contributions made by the broadleaved trees *Ulmus/Zelkova* (3.2–70.4%) and *Betula* (1.3–5%), and the herb Chenopodiaceae (0.6–54.1%).

One megathermic element (Sapindaceae), four mega-mesothermic elements (*i.e.*, *Liquidambar*, Meliaceae, *Keteleeria* and *Cedrus*), 23

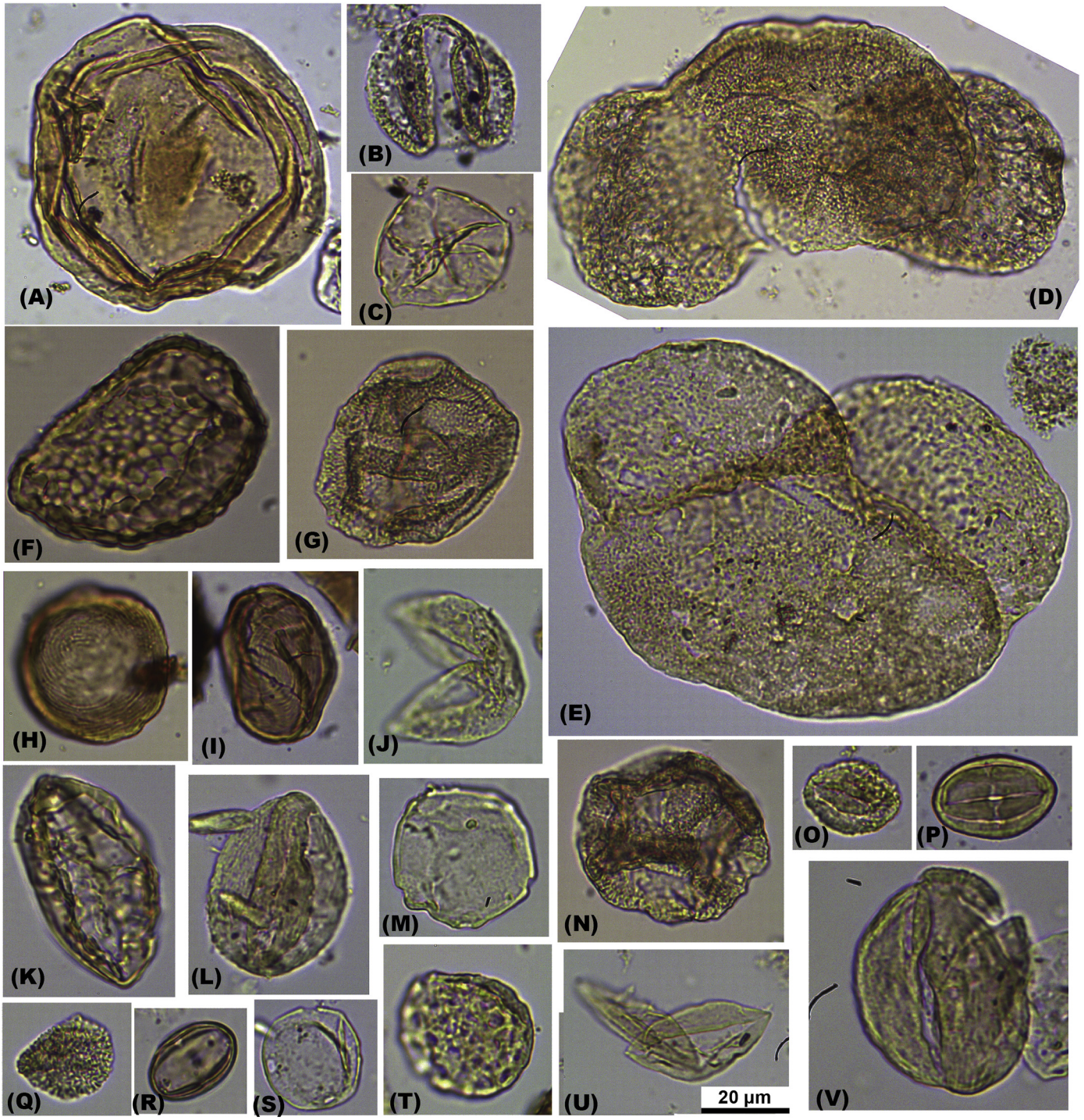

Fig. 3. Examples of taxa in the palynoassemblage. (A) *Larix*; (B) *Pinus*; (C) *Juglans*; (D) *Abies*; (E) *Picea*; (F) Polypodiaceae; (G, N) *Fupingopollenites*; (H, I) *Concentricystes*; (J, U) T-C-T (Taxodiaceae-Cupressaceae-Taxaceae); (K) *Ephedra*; (L, V) *Acer*; (M) *Pterocarya*; (O, Q) *Salix*; (P) *Rhus*; (R) Leguminosae; (S) *Celtis*; (T) Chenopodiaceae. Scale bar for all images.

mesothermic elements (*e.g.*, *Ulmus/Zelkova*, *Betula*, *Quercus* and *Carpinus*), two meso-microthermic elements (*i.e.*, *Pinus* and *Tsuga*), three microthermic elements (*i.e.*, *Abies*, *Picea* and *Larix*), one non-significant element (*i.e.*, Rosaceae), 19 herbs and shrubs (*e.g.*, Chenopodiaceae, *Ephedra*, Labiate and *Potamogeton*) were found in this zone (Table 1).

3.1.3. Zone 3

This comprises samples 1–13 inclusive (13 samples) in a 225 cm thickness of sediment. It includes 58 types of palynomorphs comprising ten gymnosperms, 46 angiosperms (18 types were herbaceous), one pteridophyte, and one alga (Table 1).

In comparison with Zone 2, the mean relative abundance of shrubby and herbaceous angiosperm pollen like Chenopodiaceae (0.3–52.9%, with a mean content of 16.8%), *Ephedra* (2%) and Poaceae (1.2%) increased. The arboreal pollen percentages for gymnosperm plants such as *Picea* (0–40.3%) and T-C-T (0.8–14.9%), and angiosperm plants such as *Ulmus/Zelkova* (0–62.2%), *Quercus* (0–8.1%) and *Betula* (1.9–21.9%) exhibited no obvious changes.

One megathermic element (*i.e.*, Sapindaceae), six mega-

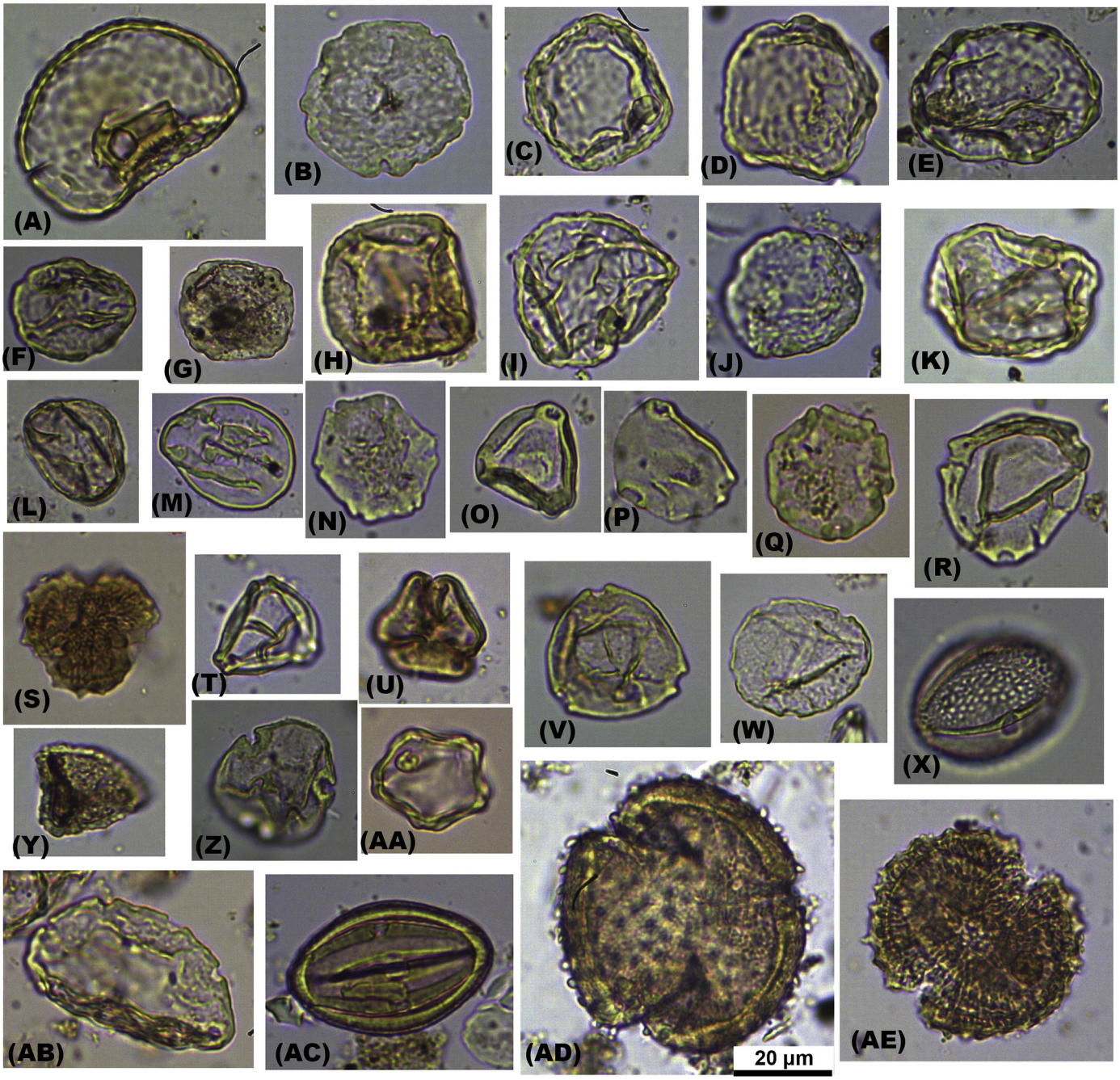

Fig. 4. Examples of taxa in the palynoassemblage. (A-K) *Ulmus/Zelkova*; (L, M) *Quercus*; (N, Q) *Pterocarya*; (O—P, R, T) *Betula*; (S, AE) Asteraceae; (U) *Koelreuteria*; (V) Betulaceae; (W, AB) *Juglans*; (X) Leguminosae; (Y) Rosaceae; (Z) *Tilia*; (AA) *Alnus*; (AC) *Nitraria*; (AD) Caprifoliaceae.

mesothermic elements (*i.e.*, *Liquidambar*, Meliaceae, Magnoliaceae, Euphorbiaceae, *Cedrus* and *Keteleeria*), 20 mesothermic elements (*e.g.*, *Ulmus/Zelkova*, *Quercus*, *Acer* and *Alnus*), two meso-microthermic elements (*i.e.*, *Pinus* and *Tsuga*), three microthermic elements (*i.e.*, *Picea*, *Abies* and *Larix*), one non-significant element (*i.e.*, Rosaceae) and 18 herbs and/or shrubs (*e.g.*, Chenopodiaceae, *Artemisia*, Poaceae and *Ephedra*) were observed in this zone (Table 1).

3.2. Climate quantification

Based on the palynomorph taxa obtained from the Caergen Section, and the climatic tolerance of their NLRs, seven climatic parameters were obtained using the CoA method (Mosbrugger and Utescher, 1997; Table 2). MAT ranged from 14.2 °C to 16.1 °C, as delimited by the presence of *Carya* and *Larix* pollen; the WMT ranged from 22.8 °C to 25.6 °C, as delimited by the presence of *Larix* and Meliaceae pollen; the CMT ranged from 1.9 °C to 7.8 °C, as delimited by the presence of *Liquidambar* and *Larix* pollen; the DT ranged from 15.5 °C to 25.5 °C, as delimited by the presence of *Nitraria* and *Keteleeria* pollen; the MAP ranged from 797.5 mm to 1113.2 mm, as delimited by the presence of *Podocarpus* and *Ephedra* pollen; the MaMP ranged from 141.5 mm to 218.8 mm, as delimited by the presence of *Carya* and *Nitraria* pollen; and the MiMP ranged from 7.2 mm to 14.1 mm, as delimited by the presence of *Ephedra* and Magnoliaceae pollen (Fig. 7, Table 2).

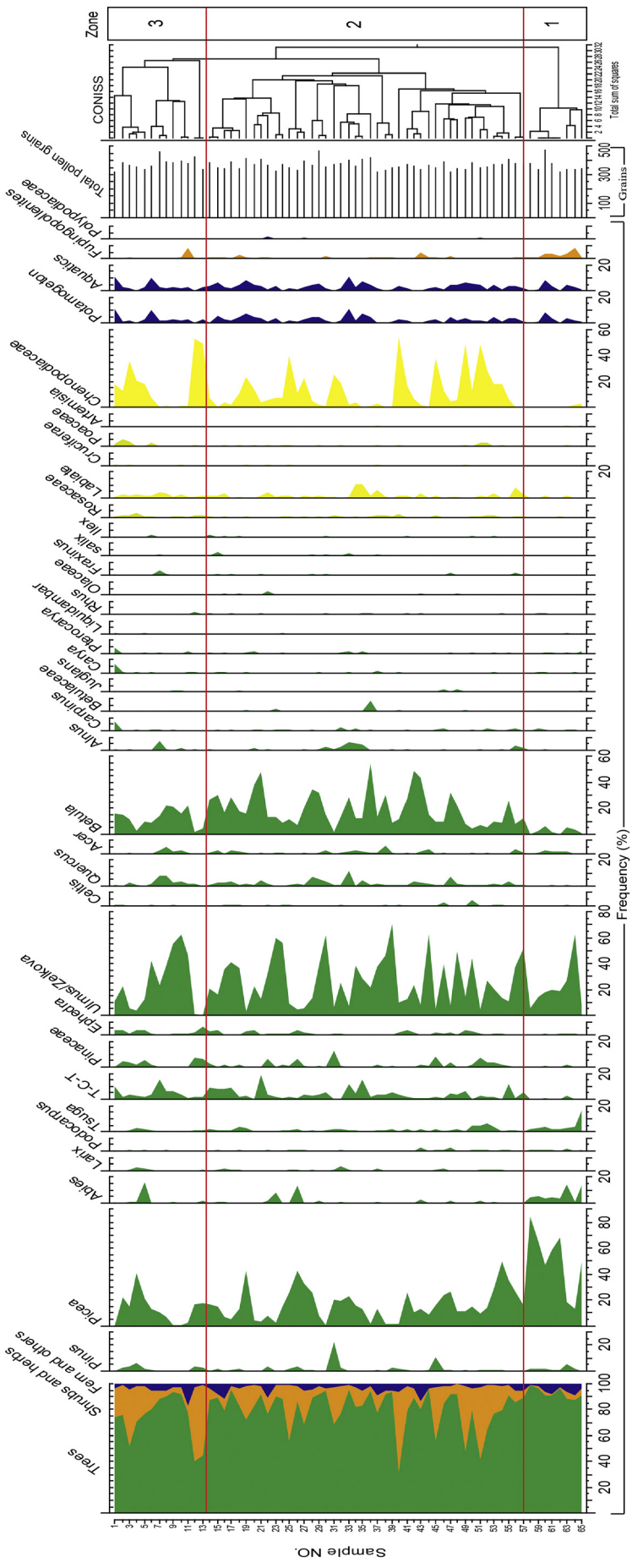

Fig. 5. Pollen diagram showing content percentage values of main taxa in samples extracted from the entire Caergen Section.

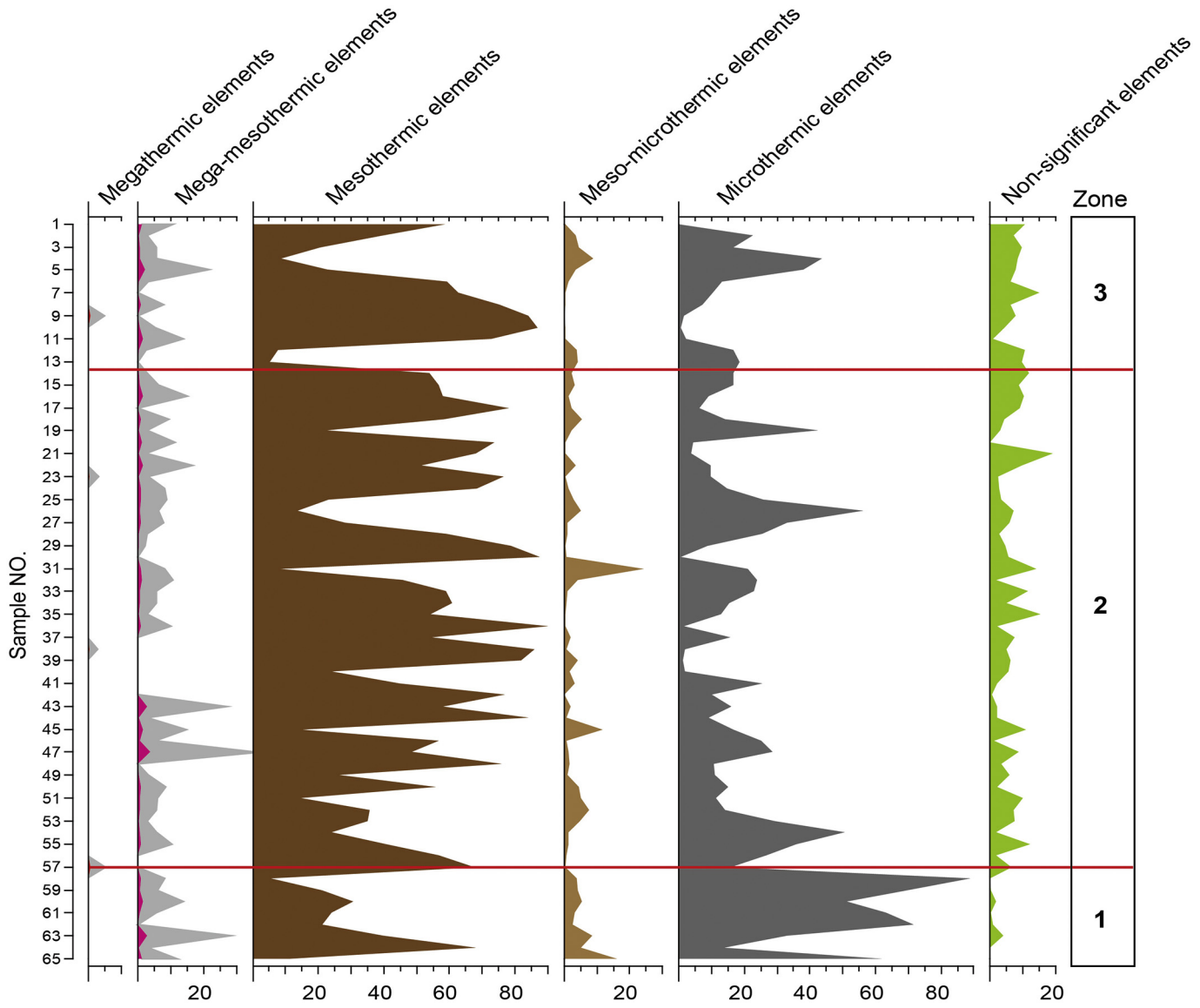

Fig. 6. Pollen synthetic diagram of the Caergen Section (light gray curves for Megathermic and Mega-mesothermic elements are 10-times exaggerated). Grouping was done regarding the ecology of the plants (see Table 1).

Table 2
A comparison of Early Miocene and present-day climatic parameters of the Zeku area, Qinghai Province.

Climatic parameters	Early Miocene	Present-day[a]
MAT (°C)	14.2–16.1 °C (mean 15.2 °C)	-2 °C
WMT (°C)	22.8–25.6 °C (mean 24.2 °C)	8.7 °C
CMT (°C)	1.9–7.8 °C (mean 4.9 °C)	−14.4 °C
DT (°C)	15.5–25.5 °C (mean 20.5 °C)	22.8 °C
MAP (mm)	797.5–1113.3 mm (mean 955.4 mm)	483.2 mm
MaMP (mm)	141.5–218.8 mm (mean 180.2 mm)	100.8 mm
MiMP (mm)	7.2–14.1 mm (mean 10.7 mm)	1.1 mm

[a] As recorded at the Zeku Meteorological Station (No. 52968; IDBMC (Information Department of Beijing Meteorological Center), 2004; 25°02′N, 101°28′E, 3662.8 m asl; data from 1971 to 2000, inclusive).

4. Palaeovegetation and palaeoclimate

4.1. Palaeovegetation

Based on the relationship between modern pollen spectra and vegetation cover, many studies have indicated that some pollen (especially bisaccate pollen such as *Pinus*, *Picea* and *Abies*) may be transported over considerable distances (Cour et al., 1999; Rousseau et al., 2008). Nevertheless, we noticed that many common and bio-sensitive plant elements were to be found in Caergen mega-fossil leaf, wood, seed and fruit flora (Guo, 1980; Li et al., 2013a, 2013b, 2014a, 2014b, 2016), *e.g.*, *Picea*, *Ulmus/Zelkova*, *Acer*, *Fraxinus*, *Pinus*, *Salix*, *Taxus*, *Ranunculus* (Ranunculaceae), Cyperaceae, *Typha*, Leguminosae and *Koelreuteria* (Sapindaceae). Of these, *Ulmus/Zelkova*, *Acer*, *Picea* and *Salix* are undoubtedly important palynofloral elements. The palynoflora of the Caergen Section can therefore be used to reconstruct the local palaeovegetation and corresponding palaeoclimate, although it may also contain some pollen from more distant provenances.

The palynological assemblage suggests that the Zeku Basin was occupied by mixed coniferous and deciduous broadleaved forests growing under warm climatic conditions during the Early to Mid-Miocene. The co-occurrence of megathermic, megathermic-mesothermic and microthermic elements would suggest the existence of vertical zonal vegetation cover on the Basin's hillsides. Microthermic and meso-microthermic species such as *Picea*, *Abies*, *Larix*, *Pinus* and *Tsuga* occupied the higher altitude slopes. Mesothermic species such as

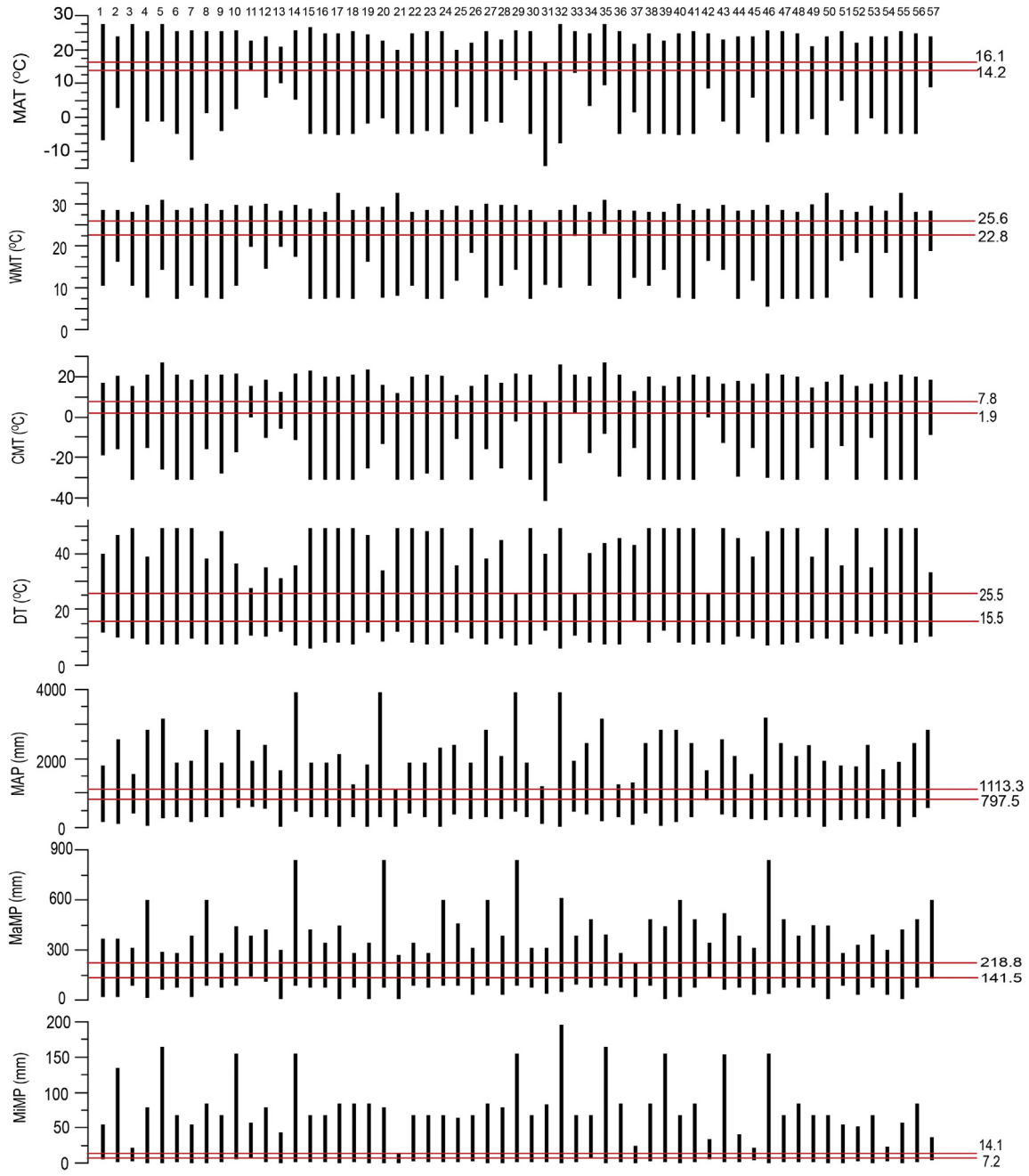

Fig. 7

Fig. 7. Coexistence intervals for Caergen section. 1. *Abies*; 2. *Acer*; 3. *Alnus*; 4. Anacardiaceae; 5. Amaranthaceae; 6. *Artemisia*; 7. *Betula*; 8. *Buxus*; 9. Caprifoliaceae; 10. *Carpinus*; 11. *Carya*; 12. *Castanea*; 13. *Cedrus*; 14. *Celtis*; 15. Chenopodiaceae; 16. Composite; 17. Cruciferae; 18. Cyperaceae; 19. Dipsaceae; 20. Elaeagnaceae; 21. *Ephedra*; 22. Ericaceae; 23. Euphorbiaceae; 24. *Fraxinus*; 25. *Ginkgo*; 26. *Humulus*; 27. *Ilex*; 28. *Juglans;* 29. *Keteleeria*; 30. Labiate; 31. *Larix*; 32. Leguminosae; 33. *Liquidambar*; 34. Magnoliaceae; 35. Meliaceae; 36. *Myriophyllum*; 37. *Nitraria*; 38. Oleaceae; 39. *Picea*; 40. *Pinus*; 41. Poaceae; 42. *Podocarpus*; 43. Polygnoaceae; 44. *Potamogeton*; 45. Pterocarya; 46. *Quercus*; 47. Ranunculaceae; 48. Rosaceae; 49. *Rhus*; 50. *Salix*; 51. Sapindaceae; 52. *Tilia*; 53. *Tsuga*; 54. *Typha*; 55. *Ulmus*; 56. Umbelliferae; 57. *Zelkova*.

Ulmus/Zelkova, *Betula*, *Quercus* and *Acer* probably grew on low altitude hillsides. Megathermic and mega-mesothermic species such as Sapindaceae, *Liquidambar*, *Keteleeria* and *Cedrus* grew sparsely in the Basin. Herbs and shrubs such as Chenopodiaceae, Labiate, Rosaceae and Poaceae covered the forest understory. Hygrophilous species such as *Salix*, *Alnus*, *Potamogeton*, Cyperaceae and *Typha* grew around lakes or wetlands (Wu et al., 1980; Hou, 1982). This palaeovegetation cover differs significantly from the present-day vegetation cover (*i.e.*, of steppe alpine meadow) in the Zeku area, where trees and shrubs have completely disappeared (Zhou et al., 1987).

Based on the three palynologic zones mentioned above, the Early to Middle Miocene vegetation succession in the Zeku Basin can be subdivided into three corresponding periods as follows (Figs. 5 and 6):

Conifers dominated the mixed coniferous and deciduous broad-leaved forest cover prevalent during Zone 1. Psychrophilous elements such as *Picea* and *Abies* dominated these forests, while typical temperate (mesothermic) elements like *Pinus*, *Ulmus/Zelkova*, *Quercus*, *Acer*, *Carpinus* and *Betula* also occupied an important place within the floral environment. Thermophilous elements such as Sapindaceae, *Liquidambar*, *Cedrus* and Meliaceae were also present. Hygrophilous

species such as *Salix*, *Fraxinus* and *Alnus* grew around palaeolakes, while aquatic plants such as *Potamogeton* and Typhaceae grew on palaeolake shores or their surrounding wetlands. Xerophilous elements such as Chenopodiaceae mainly occupied the forest understory. Compared with the other two vegetation zones, mesothermic and microthermic elements dominated Zone 1, while drought-preferring species such as Chenopodiaceae, *Ephedra* and *Nitraria* exhibited low relative abundances, indicating that this zone most likely had a relatively cool and humid climate. For the short-term variability of pollen percentages in Zone 1, the proportions of psychrophilous species *Picea* exhibit an incremental increase from bottom to top (sample nos. 65–58, Fig. 6), although the values fluctuated markedly. The percentages of thermophilic *Ulmus/Zelkova* decreased gradually. These results quite possibly indicate a stepwise cooling with large wet-cool and dry-warm climatic fluctuations under overall cool and humid climatic conditions during Zone 1.

In contrast to the conifer-dominated forests of Zone 1, mixed coniferous and deciduous broadleaved forest species dominated Zone 2. Compared with Zone 1, conifers such as *Picea* and *Abies* decreased sharply, while broadleaved trees such as *Ulmus/Zelkova*, *Betula* and *Quercus* increased dramatically. Thermophilous elements such as Sapindaceae, *Keteleeria* and *Cedrus* were also present. Xerophilous elements such as Chenopodiaceae and Labiate increased markedly and dominated the herbaceous vegetation cover. Microthermic elements increased and xerophilous elements decreased, implying that this interval was warmer and drier than the previous one. In the lower part (sample nos. 57–40, Fig. 6) of this Zone, the portions of coniferous *Picea* had a gradual reduction, while deciduous broadleaved species *Ulmus/Zelkova* and *Betula* increased gradually with large fluctuations. A large number of herbaceous Chenopodiaceae appeared suddenly and fluctuated violently. These changes of pollen percentages are probable indicative of warmer and drier climatic conditions with large dry and wet fluctuations. In the upper part (sample nos. 39–14, Fig. 6) of Zone 2, the percentages of coniferous *Picea*, deciduous broadleaved *Ulmus/Zelkova* and *Betula*, and herbaceous Chenopodiaceae fluctuated markedly, and show no obvious trend. This pattern of pollen percentages was most probably caused by cold-warm and dry-wet climate fluctuations. The almost disappearance of xerophilous Chenopodiaceae in the samples 39–33 could suggest a wetter climatic event.

During Zone 3, both microthermic elements such as *Picea*, and mesothermic elements such as *Ulmus/Zelkova* and *Betula* decreased slightly, while the xerophilous element Chenopodiaceae increased further. Taking into account the minimum relative abundance of microthermic elements (*e.g.*, *Picea*, *Abies* and *Larix*) in this period, this zone probably experienced the warmest and driest climate of all three periods. For short-term variability in pollen percentages during this Zone, the coniferous *Picea* (except samples 9–11) increased gradually, while the deciduous broadleaved *Ulmus/Zelkova* had a gradual reduction, which could indicate a warming climatic trend from bottom to top during Zone 3. High percentages of thermophilic *Ulmus/Zelkova* in combination with low psychrophilous *Picea* and raised proportions of xerophilous Chenopodiaceae in samples 9–11 point to a warm and dry climate phase.

As a general rule, this palaeovegetation succession would indicate a stepwise warming and drying trend with large dry-wet and cold-warm fluctuations from bottom to top in the Caergen Section, consistent with the upward increase in gypsum content (see Fig. 2 and Supplementary Table S1).

4.2. Palaeoclimate

Based on the palynological record, the climate parameters of Caergen section in the Early to Middle Miocene are obtained by using CoA (Table 2). When compared with modern climatic parameters recorded at the Zeku meteorological station (25°02′N, 101°28′E,3662 m asl; IDBMC (Information Department of Beijing Meteorological Center), 2004; Table 2), the mean values from the Zeku area during the Early Miocene were much higher than those of the present day, with the exception of the DT, implying a warmer and wetter climate with weaker seasonality during the Early Miocene in the Zeku Basin. For example, the MAT (ranging from 14.2 °C to 16.1 °C, with a mean value of 15.2 °C) and MAP (797.5 mm to 1113.2 mm, with a mean value of 955.4 mm) values recorded for the Early Miocene in the Zeku area were much higher than present-day ones (these being mean MAT and MAP values of −2 °C and 483.2 mm, respectively) (see Table 2). It should be mentioned that *Fupingopollenites*, an extinct palynomorph, appears intermittently throughout the pollen assemblage (Fig. 5). Using a compilation of modern climatic reconstructions and analyses, Miao et al. (2016) concluded that *Fupingopollenites* inhabited a humid, subtropical environment (*e.g.*, MAP was > 1000 mm and MAT was > 10 °C) during the Late Cenozoic, consistent with the parameters obtained here using the CoA.

Up until now, no quantitative climatic parameters have been derived from mega-fossils (*e.g.*, leaves, seeds and fruit) from this region. Nevertheless, the occurrence of mammalian fossils such as *Kubanochoerus cf. lantensis*, *Gomphoterium* and *Aprotodon* during the Miocene in the neighboring Xining Basin, and insect fossils such as *Cixius discretus* (Hemiptera, Fulgoromorpha) during the Miocene in the Zeku Basin, would suggest that this region probably experienced a warmer climate than today's, as their NLRs thrive in warm-temperate or subtropical climatic conditions (Gu et al., 1992; Qiu and Qiu, 1995; Dai et al., 2006; Li et al., 2016).

To reconstruct detailed quantitative climatic fluctuations, we applied the CoA method to each palynological Zone (*i.e.*, Zones 1–3). However, the climatic parameters for each zone were the same, except for a minor difference between the MiMPs. Low-resolution palynologic identification and minor climate change may be responsible for this situation (note that, unlike for mega-fossils, which can be identified at species level, low-resolution palynologic identification can usually only identify plants at family or genera level). However, these quantitative data at least provide a framework which indicates the existence of warmer and wetter climatic conditions than at present in the Zeku region during the Early Miocene.

5. Implications for the palaeoaltimetry of the northeastern TP

The relative abundance of conifer pollen throughout the pollen assemblage studied here is quite high, especially for *Picea* (with a mean content of 19.7%) and *Abies* (with a mean content of 1.6%). *Picea* and *Abies* are currently found on the TP at a minimum altitude of 1500 m asl, and optimally occur at altitudes ranging from 2500 to 4000 m asl, along with other high-altitude taxa such as *Tsuga* and *Cedrus* (Wu et al., 1980; Lu et al., 2008). Therefore, the appearance of *Picea* and *Abies* is often considered to have resulted from the uplift of the TP (Wang et al., 1990; Sun and Wang, 2005; Hoorn et al., 2012; Wu et al., 2014). For example, in the Xining Basin, Dupont-Nivet et al. (2008) found that the Pinaceae (and especially *Picea*) increase observed during the Late Eocene had resulted from mountain habitat formation; from this, a minimum palaeoaltitude of 1500 m asl along the Xining Basin's periphery was assumed. In the Zanda Basin, on the southwestern margins of the TP, the discovery of conifer pollen (particularly of *Picea* and *Abies*) indicated that this area's palaeoaltimetry probably did not exceed 3600 m asl (Wu et al., 2014). Modern sporopollen dispersal studies have shown that the *Pinus* pollen can be transported for distances > 1000 km by the wind, while *Picea* and *Abies* pollen are much less prone to be transported very far, as they are much heavier than *Pinus* pollen (Cour et al., 1999; Lu et al., 2008; Zhou and Li, 2011). The high percentages of *Picea* pollen observed in our samples (with a mean value of 19.7%) would suggest that the higher altitudinal areas were relatively closed to the studied area. Thus, the appearance of *Picea* in the Zeku area during the Early Miocene would probably indicate a relatively high topography (*i.e.*, a minimum of 1500 m asl) surrounded the basin.

Table 3
The Early Miocene paleoaltitude of the Zeku Basin based on plant macrofossils (Guo, 1980; Li et al., 2016) and the *TLR* method as used in this study.

Macrofossil records				*TLR* method		
Fossils	NLRs	Altitudinal range (m asl)	Paleoaltitude (m)[a]	Difference in MAT between the Early Miocene and the present day (°C)	Uplift of the Zeku Basin (m)[a]	Paleoaltitude (m)[a]
Taxus qinghaiensis	*T. chinensis*	1000–2000				
Salix sp.	*S. melea*	900–1600				
Cercis miochinensis	*C. chinensis*	250–1650	1481–1981	16.2–18.1	2218–2530	1230–1432
Podogonium oehningense	*Gleditsea heterophylla*	350–1300				
Acer subginnala	*A. ginnala*	500–1000				
Koelreuteria sp.	*K. paniculata*	300–3800				

[a] The *TLR* was 6.01 °C/km and was corrected to take account of a Miocene temperature (*T*) difference of 2.89 °C (Song et al., 2010).

Taking into account the higher temperature and the location of Zeku Basin (mid-latitude region) during Middle Miocene (Zachos et al., 2008; Song et al., 2010; Sun et al., 2015; Scotese, 2002), the coniferous taxa (*Picea* and *Abies*) should have occurred at higher elevations during the warmer climatic situations, probably would have exceeded 1500 m asl (Wu et al., 1980; Sun et al., 2015). However, the exact palaeoaltimetry of the Zeku Basin cannot be obtained based purely on pollen assemblage analysis. As we know, *T* decreases with increasing altitude (*i.e.*, the temperature lapse rate = *TLR*). Therefore, we can quantitatively estimate the degree of uplift the Basin experienced from the Early Miocene to the present day, assuming that any cooling is exclusively related to tectonic uplift. Previous studies have proposed that the Early Miocene was 2.89 °C warmer than the present day (Billups and Schrag, 2002; Wu et al., 2009; Song et al., 2010). The difference in MAT between the Early Miocene and the present day ranges from 16.2 °C to 18.1 °C (Table 3). This being the case, the cooling in *T* resulting from tectonic uplift would range from 13.31 °C to 15.21 °C. Due to a precise quantification of the lapse rates in the Miocene Zeku Basin is impossible, and thus the accurate palaeoaltitude can't be directly calculated from ancient lapse rates. Under the circumstances, the cross-validation from different evidences and methods may be one of the most effective approaches. Therefore, the recently published Miocene *TLR* (Song et al., 2010) was applied here, in combination with the megafossils flora from the bottom of Caergen Section (Fig. 2), to reconstruct the Zeku Basin's Miocene palaeoaltitude. Taking the *TLR* to be 6.01 °C/1000 m (Song et al., 2010), the Zeku Basin may have experienced an uplift of 2218–2530 m between the Early Miocene and the present day. Thus, the palaeoaltitude of the Zeku Basin could be calculated to have been between 1230 m asl and 1432 m asl (the present-day mean altitude is 3700 m asl), with a minimum palaeoaltitude of 1500 m asl along the Basin's periphery during the Early Miocene. The occurrence of plant macrofossils such as *Taxus qinghaisis*, *Salix* sp., *Cercis miochinensis*, *Podogonium oehningense* and *Acer subginnala* in the oil shale layer (Fig. 2) would indicate that the mean altitude of the Zeku Basin was ~1000–1500 m asl during the Early Miocene (Guo, 1980; Li et al., 2016; Table 3). Although being just a rough estimation, our results are consistent with this conclusion.

Over recent years, many divergent hypotheses regarding the uplift history of the northern TP have been proposed. Some studies have held that the TP reached its present-day altitude during the Oligocene or Eocene (Quade et al., 2011; Rowley and Currie, 2006; Rowley and Garzione, 2007; Garzione, 2008). Others have suggested that the TP gained its present-day altitude during the Early Miocene or Late Oligocene, as recorded by the eolian sedimentary record on the Chinese Loess Plateau (CLP; Guo et al., 2002; Qiang et al., 2011).

Our estimates of the palaeoaltimetry of the Zeku Basin suggest a palaeoaltitude of 1200–1400 m asl during the Early Miocene, close to the altitude of 1300–2900 m asl for the Early Miocene Wudaoliang Basin, northern TP, and based on *Berberis* leaf fossil analyses (Sun et al., 2015). Our finding does not support the view that the TP gained its present-day altitude prior to the Miocene (Quade et al., 2011; Guo et al., 2002; Rowley and Currie, 2006; Garzione, 2008; Qiang et al., 2011), but rather, and similar to the predictions made by stepwise uplift models, that the northern TP achieved its present-day altitude after the Miocene (Tapponnier et al., 2001).

6. Conclusions

1) Palynological data from the Caergen Section in the Zeku Basin are dominated by angiosperm pollen (with a mean content of 64.2%), followed by gymnosperm pollen (with a mean content of 31.7%) and pteridophyte spores (with a mean content of 0.2%).
2) The vegetation cover in the Zeku Basin during the Early Miocene was composed of mixed temperate coniferous (*e.g.*, *Picea*, *Abies* and *Tsuga*) and deciduous broadleaved (*e.g.*, *Ulmus/Zelkova*, *Betula* and *Quercus*) forests, with some subtropical elements (*e.g.*, *Carya* and *Liquidambar*). This vegetation cover suggests a warm, temperate climate.
3) Palaeoclimatic parameters for the Zeku Basin were obtained using the CoA method; the results indicate a much warmer and more humid climate during the late Early Miocene than today, with MAT 14.2–16.1 °C and MAP 797.5–1113.2 mm.
4) Based on the difference in temperature between the Early Miocene and the present day, a probable palaeoaltitude of 1200–1400 m asl was estimated for the Zeku Basin during the Early Miocene, suggesting that this Basin has most likely experienced a degree of uplift within the range of 2200–2500 m since the Early Miocene.

Supplementary data to this article can be found online at https://doi.org/10.1016/j.palaeo.2018.09.009.

Acknowledgments

This work was co-supported by the State Program of the National Natural Science Foundation of China (grant no. 41330745), the National Natural Science Foundation of China (grant nos. 41877445, 41202008, 41771209 and 41872017), and the Foundation of the State Key Laboratory of Palaeobiology and Stratigraphy (Nanjing Institute of Geology and Palaeontology, Chinese Academy of Sciences (CAS)) (Grant No. 153108), and the Fundamental Research Funds for Central Universities (grant nos. lzujbky-2017-216 and 310827172005). We highly appreciate the willingness to review this paper and the valuable comments by T. Utescher and a second anonymous reviewer. Special thanks to Editor Howard Falcon-Lang for his constructive suggestions and help with English improvement on this paper.

References

An, Z.S., Kutzbach, J.E., Prell, W.L., Porter, S.C., 2001. Evolution of Asian monsoons and phased uplift of the Himalaya–Tibetan plateau since Late Miocene times. Nature 411, 62–66.

Billups, K., Schrag, D.P., 2002. Palaeotemperatures and ice volume of the past 27 Myr revisited with paired Mg/Ca and $^{18}O/^{16}O$ measurements on benthic foraminifera.

Palaeoceanography 17, 1003.
Boos, W.R., Kuang, Z.M., 2010. Dominant control of the South Asian monsoon by orographic insulation versus plateau heating. Nature 463, 218–222.
Bruch, A.A., Zhilin, S.G., 2007. Early Miocene climate of Central Eurasia — evidence from Aquitanian Floras of Kazakhstan. Palaeogeogr. Palaeoclimatol. Palaeoecol. 248, 32–48.
Chaloner, W.G., Creber, G.T., 1990. Do fossil plants give a climatic signal? J. Geol. Soc. Lond. 147, 343–350.
Cour, P., Zheng, Z., Duzer, D., Callejaa, M., Yao, Z., 1999. Vegetational and climatic significance of modern pollen rain in northwestern Tibet. Rev. Palaeobot. Palynol. 104, 183–204.
Currie, B.S., Rowley, D.B., Tabor, N.J., 2005. Middle Miocene palaeoaltimetry of southern Tibet: implications for the role of mantle thickening and delamination in the Himalayan orogen. Geology 33, 181.
Dai, S., Fang, X.M., Dupont-Nivet, G., Song, C.H., Gao, J.P., Krijgsman, W., Langereis, C., Zhang, W.L., 2006. Magnetostratigraphy of Cenozoic sediments from the Xining Basin: tectonic implications for the northeastern Tibetan Plateau. J. Geophys. Res. 111, B11102. https://doi.org/10.1029/2005JB004187.
Decelles, P.G., Quade, J., Kapp, P., Fan, M., Dettman, D.L., Ding, L., 2007. High and dry in central Tibet during the Late Oligocene. Earth Planet. Sci. Lett. 253, 389–401.
Deng, T., Li, Q., Tseng, Z.J., Takeuchi, G.T., Wang, Y., Xie, G.P., Wang, S.Q., Hou, S.K., Wang, X.M., 2012. Locomotive implication of a Pliocene three-toed horse skeleton from Tibet and its palaeo-altimetry significance. Proc. Natl. Acad. Sci. 109 (19), 7374–7378.
Dong, M., Fang, X.M., Shi, Z.T., Min, Q.Z., Su, H., 2011. Early Pleistocene lacustrine spore-pollen records and evolution of palaeoclimatie in Linxia Basin, Gansu Province, China. Quaternary Sciences 31 (1), 104–111 (in Chinese with English abstract).
Dupont-Nivet, G., Hoorn, C., Konert, M., 2008. Tibetan uplift prior to the Eocene-Oligocene climate transition: evidence from pollen analysis of the Xining Basin. Geology 36 (12), 987–990.
Fang, J., Wang, Z., Tang, Z., 2009. (Eds.). Atlas of Woody Plants in China, Distribution and Climate. vols. 1, 2 & 3. Higher Education Press, Beijing, pp. 1–1908.
Fang, X.M., Song, C.H., Dai, S., Zhu, Y.T., Gao, J.P., Zhang, W.L., 2007. Cenozoic deformation and uplift of the NE Qinghai-Tibet Plateau: evidence from high-resolution magnetostratigraphy and basin evolution. Earth Science Frontier 14, 230–242 (China University of Geosciences, Bejing; Peking University; in Chinese with English Abstract).
Fang, X.M., Yan, M.D., Van der Voo, R., Rea, D.K., Song, C.H., Parés, J.M., Gao, J.P., Nie, J.S., Dai, S., 2005. Late Cenozoic deformation and uplift of the NE Tibetan Plateau: evidence from high-resolution magnetostratigraphy of the Guide Basin, Qinghai Province, China. Geol. Soc. Am. Bull. 117, 1208–1225.
Garzione, C.N., 2008. Surface uplift of Tibet and Cenozoic global cooling. Geology 36 (12), 1003–1004.
Garzione, C.N., Quade, J., Decelles, P.G., English, N.B., 2000. Predicting palaeoelevation of Tibet and the Himalaya from $\delta^{18}O$ vs. altitude gradients in meteoric water across the Nepal Himalaya. Earth Planet. Sci. Lett. 183, 215–229.
Grimm, E.C., 1991. Tilia Version 2.0. Illinois State Museum, Research and Collections Centre.
Grimm, E., 2011. Tilia Software V. 1.7. 16. Illinois State Museum, Springfield.
Grimm, G., Denk, T., 2012. Reliability and resolution of the Coexistence Approach – a revalidation using modern-day data. Rev. Palaeobot. Palynol. 17, 33–47.
Grimm, G.W., Bouchal, J.M., Denk, T., Potts, A., 2016. Fables and foibles: a critical analysis of the Palaeoflora database and the Coexistence Approach for palaeoclimate reconstruction. Rev. Palaeobot. Palynol. 233, 216–235.
Grimm, G.W., Potts, A.J., 2016. Fallacies and fantasies: the theoretical underpinnings of the Coexistence Approach for palaeoclimate reconstruction. Clim. Past 12, 611–622.
Gu, Z.G., Bai, S.H., Zhang, X.T., Ma, Y.Z., Wang, S.H., Li, B.Y., 1992. Neogene subdivision and correlation of sediments within the Guide and Hualong basins of Qinghai province. J. Stratigr. 16, 96–104 (in Chinese with English abstract).
Guo, S.X., 1980. Miocene flora of Zeku County, Qinghai. Acta Palaeontol. Sin. 19, 406–412 (in Chinese with English abstract).
Guo, Z.T., Ruddiman, W.F., Hao, Q.Z., Wu, H.B., Qiao, Y.S., Zhu, R.X., Peng, S.Z., Wei, J.J., Yuan, B.Y., Liu, T.S., 2002. Onset of Asian desertification by 22 Myr ago inferred from Loess Deposits in China. Nature 416, 159–163.
Hoorn, C., Straathof, J., Abels, H.A., Xu, Y., Utescher, T., Dupont-Nivet, G., 2012. A late Eocene palynological record of climate change and Tibetan Plateau uplift (Xining Basin, China). Palaeogeogr. Palaeoclimatol. Palaeoecol. 344-345, 16–38.
Hou, X.Y., 1982. Vegetation Geography of China with Reference to the Chemical Composition of Dominant Plants. Science Press, Beijing (in Chinese).
Hsu, H.H., Liu, X., 2003. Relationship between the Tibetan Plateau heating and East Asian summer monsoon rainfall. Geophys. Res. Lett. 30 (200), 2066.
Hui, Z.C., Li, J.J., Xu, Q.H., Song, C.H., Zhang, J., Wu, F.L., Zhao, Z.J., 2011. Miocene vegetation and climatic changes reconstructed from a sporopollen record of the Tianshui Basin, Ne Tibetan Plateau. Palaeogeogr. Palaeoclimatol. Palaeoecol. 308, 373–382.
IDBMC (Information Department of Beijing Meteorological Center), 2004. Land Climate Data of China (1971–2000) (Part II). China Meteorological Press, Beijing (in Chinese).
Jiménez-Moreno, G., 2006. Progressive substitution of a subtropical forest for a temperate one during the middle Miocene climate cooling in Central Europe according to palynological data from cores Tengelic-2 and Hidas-53 (Pannonian Basin, Hungary). Rev. Palaeobot. Palynol. 142, 1–14.
Kou, X.Y., Ferguson, D.K., Xu, J.X., Wang, Y.F., Li, C.S., 2006. The reconstruction of palaeovegetation and palaeoclimate in the late Pliocene of West Yunnan, China. Clim. Chang. 77, 431–448.
Kutzbach, J.E., Guetter, P.J., Ruddiman, W.F., 1989. The sensitivity of climate to late Cenozoic uplift in Southeast Asia and the American southwest: numerical experiments. J. Geophys. Res. 94, 18393–18407.
Lease, R.O., Burbank, D.W., Gehrels, G.E., Wang, Z., Yuan, D., 2007. Signatures of mountain building; detrital zircon U/Pb ages from northeastern Tibet. Geology (Boulder) 35 (3), 239–242.
Li, J.F., Ferguson, D.K., Yang, J., Feng, G.P., Ablaev, A.G., Wang, Y.F., Li, C.S., 2009. Early Miocene vegetation and climate in Weichang District, North China. Palaeogeogr. Palaeoclimatol. Palaeoecol. 280, 47–63.
Li, J.J., 1995. Uplift of Qinghai-Xizang (Tibet) Plateau and Global Change. Lanzhou University Press, Lanzhou.
Li, J.J., Fang, X.M., Song, C.H., Pan, B.T., Ma, Y.Z., Yan, M.D., 2014a. Late Miocene–Quaternary rapid stepwise uplift of the NE Tibetan Plateau and its effects on climatic and environmental changes. Quat. Res. 81, 400–423.
Li, J.J., Feng, Z.D., 1988. Late Quaternary monsoon patterns on the loess plateau of China. Earth Surf. Process. Landf. 13, 125–135.
Li, S., Xing, Y., Valdes, P.J., Huang, Y., Su, T., Farnsworth, A., Lunt, D.J., Tang, H., Kennedy, A.T., Zhou, Z., 2018. Oligocene climate signals and forcings in Eurasia revealed by plant macrofossil and modelling results. Gondwana Res. 61, 115–127.
Li, X.C., He, W.L., Xiao, L., Yang, H.Y., Xie, S.P., 2013a. The restudy on the Miocene flora of Zeku, Qinghai. In: The 27th Annual Conference Proceedings of the Palaeontological Society of China (PSC) and the 11th National Congress of PSC, Dongyang, Zhejiang Province, Chinapp. 190 (in Chinese).
Li, X.C., Li, Z.W., Xiao, L., Yang, H.Y., He, W.L., Yao, Y.Z., Yang, Q., Ren, D., 2014b. The Miocene palaeobiota of Zeku, Qinghai and its palaeoclimate. In: 2014 Annual Conference Proceedings of the Palaeobotanical Branch of the Palaeontological Society of China. Sun Yat-Sen University, Guangzhou, Chinapp. 32 (in Chinese).
Li, X.C., Sun, B.N., Xiao, L., Wu, J.Y., Ding, S.T., Jia, H., 2013b. Legume fruits from the Miocene of eastern Zhejiang and Qinghai, China. In: 2013 Annual Conference Proceedings of the Palaeobotanical Branch of the Palaeontological Society of China. Lanzhou University, Lanzhou, Chinapp. 49–50.
Li, X.C., Xiao, L., Lin, Z.C., He, W.L., Yang, Q., Yao, Y.Z., Ren, D., Guo, J.F., Guo, S.X., 2016. Fossil fruits of *Koelreuteria* (Sapindaceae) from the Miocene of Northeastern Tibetan Plateau and their palaeoenvironmental, phytogeographic and phylogenetic implications. Rev. Palaeobot. Palynol. 234, 125–135.
Liang, M.M., Bruch, A., Collinson, M., Mosbrugger, V., Li, C.S., Sun, Q.G., Hilton, J., 2003. Testing the climatic estimates from different palaeobotanical methods: an example from the Middle Miocene Shanwang flora of China. Palaeogeogr. Palaeoclimatol. Palaeoecol. 198, 279–301.
Lu, H.Y., Wu, N.Q., Yang, X.D., Shen, C.M., Zhu, L.P., Wang, L., Li, Q., Xu, D.K., Tong, G.B., Sun, X.J., 2008. Spatial pattern of Abies and Picea surface pollen distribution along the elevation gradient in the Qinghai–Tibetan Plateau and Xinjiang, China. Boreas 37, 254–262.
Ma, Y.Z., Fang, X.M., Li, J.J., Wu, F.L., Zhang, J., 2005. The vegetation and climate change during the Neocene and Early Quaternary in the Jiuxi Basin, China. Sci. China Ser. D Earth Sci. 5, 676–688.
Ma, Y.Z., Li, J.J., Fang, X.M., 1998. Pollen assemblage in 30.6–5.0 Ma redbeds of Linxia region and climate evolution. Chin. Sci. Bull. 43, 301–304.
Manabe, S., Terpstra, T.B., 1974. The effects of mountains on the general circulation of the atmosphere as identified by numerical experiments. J. Atmos. Sci. 31, 3–42.
Meyer, B., Tapponnier, P., Bourjot, L., Métivier, F., Gaudemer, Y., Peltzer, G., Guo, S., Chen, Z., 1998. Crustal thickening in Gansu-Qinghai, lithospheric mantle subduction, and oblique, strike-slip controlled growth of the Tibet plateau. Geophys. J. Int. 135, 1–47.
Miao, Y.F., Fang, X.M., Wu, F.L., Cai, M.T., Song, C.H., Meng, Q.Q., Xu, L., 2013. Late Cenozoic continuous aridification in the Western Qaidam Basin: evidence from sporopollen records. Clim. Past 9, 1863–1877.
Miao, Y.F., Song, C.H., Fang, X.M., Meng, Q.Q., Zhang, P., Wu, F.L., Yan, X.L., 2016. Late Cenozoic genus *Fupingopollenites* development and its implications for the Asian summer monsoon evolution. Gondwana Res. 29, 320–333.
Molnar, P., 2005. Mio-Pliocene growth of the Tibetan Plateau and evolution of East Asian climate. Palaeontol. Electron. 8 (1), 1–23.
Molnar, P., Boos, W.R., Battisti, D.S., 2010. Orographic controls on climate and palaeoclimate of Asia: thermal and mechanical roles for the Tibetan Plateau. Annu. Rev. Earth Planet. Sci. 38 (1), 77–102.
Mosbrugger, V., 1999. The nearest living relative method. In: Jones, T.P., Rowe, N.P. (Eds.), Fossil Plants and Spores Modern Techniques. Geological Society, London, pp. 261–265.
Mosbrugger, V., Utescher, T., 1997. The coexistence approach - a method for quantitative reconstructions of tertiary terrestrial palaeoclimate data using plant fossils. Palaeogeogr. Palaeoclimatol. Palaeoecol. 134, 61–86.
Mosbrugger, V., Utescher, T., Dilcher, D.L., 2005. Cenozoic continental climatic evolution of Central Europe. Proc. Natl. Acad. Sci. 102 (42), 14964–14969.
Prasad, V., Utescher, T., Sharma, A., Singh, I.B., Garg, R., Gogoi, B., Srivastava, J., Uddandam, P.R., Joachimskif, M.M., 2018. Low-latitude vegetation and climate dynamics at the Paleocene-Eocene transition – a study based on multiple proxies from the Jathang section in northeastern India. Palaeogeogr. Palaeoclimatol. Palaeoecol. 497, 139–156.
Qiang, X., An, Z., Song, Y., Chang, H., Sun, Y., Liu, W., A, H., Dong, J., Fu, C., Wu, F., Lu, F., Cai, Y., Zhou, W., Cao, J., Xu, X., Ai, L., 2011. New eolian red clay sequence on the western Chinese Loess Plateau linked to onset of Asian desertification about 25 Ma ago. Sci. China Ser. D Earth Sci. 54, 136–141.
Qiu, Z.D., Qiu, Z.X., 1995. Chronological sequence and subdivision of Chinese Neogene. Palaeogeogr. Palaeoclimatol. Palaeoecol. 116, 41–70.
Quade, J., Breecker, D.O., Daeron, M., Eiler, J., 2011. The palaeoaltimetry of Tibet: an isotopic perspective. Am. J. Sci. 311, 77–115.
Quan, C., Liu, Y.S., Utescher, T., 2012. Eocene monsoon prevalence over China: a

palaeobotanical perspective. Palaeogeogr. Palaeoclimatol. Palaeoecol. 365-366, 302–311.
Rousseau, D.D., Schevin, P., Ferrier, J., Jolly, D., Andreasen, T., Ascanius, S.E., Hendriksen, S.E., Poulsen, U., 2008. Long-distance pollen transport from North America to Greenland in Spring. J. Geophys. Res. 113, G02013. https://doi.org/10.1029/2007JG000456.
Rowley, D.B., Currie, B.S., 2006. Palaeo-altimetry of the late Eocene to Miocene Lunpola Basin, central Tibet. Nature 439, 677–681.
Rowley, D.B., Garzione, C.N., 2007. Stable isotope-based palaeoaltimetry. Annu. Rev. Earth Planet. Sci. 35, 463–508.
Rowley, D.B., Pierrehumbert, R.T., Currie, B.S., 2001. A new approach to stable isotope-based palaeoaltimetry: implications for palaeoaltimetry and palaeohypsometry of the High Himalaya since the Late Miocene. Earth Planet. Sci. Lett. 188, 253–268.
Ruddiman, W.F., Kutzbach, J.E., 1989. Forcing of late Cenozoic Northern Hemisphere climate by plateau uplift in southern Asia and the American West. J. Geophys. Res. 94 (D15), 18409–18427.
Scotese, C.R., 2002. PALEOMAP. website. http://www.scotese.com.
SCQPWG (Stratigraphic Charts of Qinghai Province Writing Group), 1980. Regional Stratigraphic Chart of Northwest China: Vol. Geological Publishing House, Beijing, Qinghai Province.
Song, X.Y., Spicer, R.A., Yang, J., Yao, Y.F., Li, C.S., 2010. Pollen evidence for an Eocene to Miocene elevation of central southern Tibet predating the rise of the High Himalaya. Palaeogeogr. Palaeoclimatol. Palaeoecol. 297, 159–168.
Song, Z.C., Zheng, Y.H., Li, M.Y., Zhang, Y.Y., Wang, W.M., Wang, D.N., Zhao, C.B., Zhou, S.F., Zhu, Z.H., Zhao, Y.N. (Eds.), 1999. The Late Cretaceous and Tertiary Spores and Pollen. Fossil Spores and Pollen of China. vol. 1. Science Press, Beijing, pp. 1–910 (Eds.). (in Chinese with English summary).
Srivastava, G., Paudayal, K.N., Utescher, T., Mehrotra, R.C., 2018. Miocene vegetation shift and climate change: evidence from the Siwalik of Nepal. Glob. Planet. Chang. 161, 108–120.
Sun, B., Wang, Y.F., Li, C.S., Yang, J., Li, J.F., Li, Y.L., Deng, T., Wang, S.Q., Zhao, M., Spicer, R.A., Ferguson, D.K., Mehrotra, R.C., 2015. Early Miocene elevation in Northern Tibet estimated by palaeobotanical evidence. Sci. Rep. 5, 10379. https://doi.org/10.1038/srep10379.
Sun, X.J., Wang, P.X., 2005. How old is the Asian monsoon system? Palaeobotanical Records from China. Palaeogeogr. Palaeoclimatol. Palaeoecol. 222, 181–222.
Tapponnier, P., Xu, Z., Roger, F., Meyer, B., Arnaud, N., Wittlinger, G., Yang, J., 2001. Oblique stepwise rise and growth of the Tibet plateau. Science 294, 1671–1677.
Utescher, T., Mosbrugger, V., 1997–2012. PALAEOFLORA Database. http://www.palaeoflora.de/.
Utescher, T., Bruch, A.A., Erdei, B., François, L., Ivanov, D., Jacques, F.M.B., Kern, A.K., Liu, Y.S.C., Mosbrugger, V., Spicer, R.A., 2014. The coexistence approach–theoretical background and practical considerations of using plant fossils for climate quantification. Palaeogeogr. Palaeoclimatol. Palaeoecol. 410, 58–73.
Utescher, T., Bruch, A.A., Micheels, A., Mosbrugger, V., Popova, S., 2011. Cenozoic climate gradients in Eurasia – a palaeo-perspective on future climate change? Palaeogeogr. Palaeoclimatol. Palaeoecol. 304, 351–358.
Vieira, M., Pound, M.J., Pereira, D.I., 2018. The late Pliocene palaeoenvironments and palaeoclimates of the western Iberian Atlantic margin from the Rio Maior flora. Palaeogeogr. Palaeoclimatol. Palaeoecol. 495, 245–258.
Wang, D.N., Sun, X.Y., Zhao, Y.N., He, Z.S., 1990. Palynoflora From Late Cretaceous to Tertiary in Some Regions of Qinghai and Xinjiang. China Environmental Science Press, Beijing, pp. 1–179 (in Chinese with English abstract).
Wang, F., Qian, N.F., Zhang, Y.L., Yang, H.Q., 1995. Pollen Flora of China, 2nd ed. Science Press, Beijing, pp. 1–461 (in Chinese).
Wang, H.S., 1992. Floristic Phytogeography. Science Press, Beijing, pp. 1–180.
Wang, W.M., 1994. Paleofloristic and paleoclimatic implications of Neogene palynofloras in China. Rev. Palaeobot. Palynol. 82, 239–250.
Wang, W.M., Deng, T., 2009. Palynoflora from stratotype section of the Neogene Xiejia stage and its significance. Acta Palaeontol. Sin. 48 (1), 1–8 (in Chinese with English abstract).
Wang, X.X., Zattin, M., Li, J.J., Song, C.H., Peng, T.J., Liu, S.P., Liu, B., 2011. Eocene to Pliocene exhumation history of the Tianshui-Huicheng region determined by apatite fission track thermochronology: implications for evolution of the Northeastern Tibetan Plateau Margin. J. Asian Earth Sci. 42, 97–110.
Wang, Z.C., Zhang, P.Z., Carmala, N.G., Richard, O.L., Zhang, G.L., Zheng, D.W., Brian, H., Yuan, D.Y., Li, C.Y., Liu, J.H., Wu, Q.L., 2012. Magnetostratigraphy and depositional history of the Miocene Wushan Basin on the Ne Tibetan Plateau, China: implications for Middle Miocene tectonics of the West Qinling Fault Zone. J. Asian Earth Sci. 44, 189–202.
Wu, F.L., Fang, X.M., Miao, Y.F., Dong, M., 2010. Environmental indicators from comparison of sporopollen in Early Pleistocene lacustrine sediments from different climatic zones. Chin. Sci. Bull. 55 (26), 2981–2988.
Wu, F.L., Herrmann, M., Fang, X.M., 2014. Early Pliocene palaeo-altimetry of the Zanda Basin indicated by a sporopollen record. Palaeogeogr. Palaeoclimatol. Palaeoecol. 412, 261–268.
Wu, Y.S., 2001. Palynoflora from the Late Miocene-Early Pliocene from the Leijiahe Section, Lingtai, Gansu Province, China. Acta Bot. Sin. 43 (7), 750–756 (Chinese with English abstract).
Wu, Z., Wu, Z., Ye, P., Hu, D., Peng, H., 2006. Late Cenozoic environmental evolution of the Qinghai-Tibet Plateau as indicated by the evolution of sporopollen assemblages. Geol. China 33 (5), 967–979 (Chinese with English abstract).
Wu, Z.H., Wu, Z.H., Ye, P.S., Hu, D.G., Peng, H., 2009. Oligocene thrust systems in central Tibetan Plateau. Geol. China 38, 522–536 (In Chinese with English abstract).
Wu, Z.Y., Wang, X.F., Liu, F.Y., Zhu, Y.C., Li, S.Y., Li, B., He, S.Y., Zhang, X.S., Chen, C.D., Zhou, Y.L., Zhou, G.Y., Lin, Y., Hou, X.Y., 1980. Vegetation of China. Science Press, Beijing (in Chinese).
Xing, Y.W., Utescher, T., Jacques, F.M.B., Su, T., Liu, Y.C., Huang, Y.J., Zhou, Z.K., 2012. Palaeoclimatic estimation reveals a weak winter monsoon in Southwestern China during the Late Miocene: evidence from plant macrofossils. Palaeogeogr. Palaeoclimatol. Palaeoecol. 358-360, 19–26.
Xu, J.X., Ferguson, D.K., Li, C.S., Wang, Y.F., 2008. Late Miocene vegetation and climate of the Lühe Region in Yunnan, Southwestern China. Rev. Palaeobot. Palynol. 148, 36–59.
Yang, J., Wang, Y.F., Spicer, R.A., Mosbrugger, V., Li, C.S., Sun, Q.G., 2007. Climatic reconstruction at the Miocene Shanwang Basin, China, using leaf margin analysis, clamp, coexistence approach, and overlapping distribution analysis. Am. J. Bot. 94 (4), 599–608.
Yao, Y.F., Bruch, A.A., Mosbrugger, V., Li, C.S., 2011. Quantitative reconstruction of Miocene climate patterns and evolution in Southern China based on plant fossils. Palaeogeogr. Palaeoclimatol. Palaeoecol. 304, 291–307.
Yin, A., Harrison, T.M., Ryerson, F.J., Chen, W., Kidd, W.S.F., Copeland, P., 1994. Tertiary structural evolution of the Gangdese thrust system, southeastern Tibet. J. Geophys. Res. 99, 18175–18201.
Young, C.C., 1975. Feathers in the oil-bearing shales from the Tse-Ku-Tsa-Ka, Qinghai. Vertebrata Palasiatica 13, 163–165 (Chinese with English Abstract).
Zachos, J.C., Dickens, G.R., Zeebe, R.E., 2008. An early Cenozoic perspective on greenhouse warming and carbon-cycle dynamics. Nature 451, 279–283.
Zhang, Q.Q., Ferguson, D.K., Mosbrugger, V., Wang, Y.F., Li, C.S., 2012. Vegetation and climatic changes of SW China in response to the uplift of Tibetan Plateau. Palaeogeogr. Palaeoclimatol. Palaeoecol. 363–364, 23–36.
Zhou, X.M., Wang, Z.B., Du, Q., 1987. Vegetation of Qinghai Province. Qinghai People's Press, Xining (in Chinese).
Zhou, X.X., Li, X.Q., 2011. Variations in spruce (*Picea* sp.) distribution on the Chinese Loess Plateau and surrounding areas during the Holocene. The Holocene (special issue) 1–10. https://doi.org/10.1177/0959683611400195.